

# Cloud-Point Curves of Polymer Solutions from Thermo-optical Measurements

Y. C. Bae, S. M. Lambert, D. S. Soane, and J. M. Prausnitz\*

Department of Chemical Engineering, University of California and Chemical Sciences Division, Lawrence Berkeley Laboratory, Berkeley, California 94720

Received November 27, 1990; Revised Manuscript Received February 25, 1991

**ABSTRACT:** Thermo-optical analysis (TOA) provides a simple, rapid, and reliable experimental method to determine cloud-point curves of binary polymer/solvent systems. Phase diagrams have been obtained for different molecular weights of polystyrene in cyclohexane, methyl acetate, ethyl acetate, and *tert*-butyl acetate and for poly(ethylene glycol) in water. Polystyrene solutions exhibit both upper and lower critical solution temperatures, while aqueous poly(ethylene glycol) solutions give closed-loop phase diagrams. The TOA apparatus described here uses very small samples (0.02 cm<sup>3</sup>); for a binary system, upper and lower cloud-point curves can easily be obtained in ~8 h.

## Introduction

This work discusses a simple and efficient thermo-optical analysis apparatus for measuring liquid-liquid equilibria in binary systems containing a solvent and an essentially monodisperse polymer.

Cloud-point curves of many polymer/solvent systems have been measured for the past several decades. Polystyrene/cyclohexane is one of the well-known systems that has both an upper critical solution temperature (UCST) and a lower critical solution temperature (LCST).<sup>1-3</sup> UCST and LCST have been reported for a variety of binary systems, e.g., cellulose acetate/acetone,<sup>4</sup> polyisobutylene/benzene,<sup>5,6</sup> and polystyrene/methylcyclohexane.<sup>7</sup> There are many binary systems that show either UCST or LCST, e.g., polyethylene/*n*-pentane,<sup>7</sup> polymethylene solutions,<sup>8</sup> polyisobutylene/isopentane,<sup>9</sup> and polypropylene oxide/*n*-pentane.<sup>9</sup> Compilations of experimental results are given, for example, in refs 10 and 11.

Immiscibility occurs if the temperature of the polymer solution is raised above the LCST or lowered below the UCST. Increasing the molecular weight of the polymer raises the UCST and lowers the LCST, thus shrinking the region of complete miscibility. Both UCST and LCST are often observed in polymer solutions.<sup>12</sup>

For a polymer in a poor solvent, the typical hourglass type of cloud-point curve is often observed, as for example, for polystyrene/acetone<sup>13</sup> and for poly(ethylene glycol)/*tert*-butyl acetate.<sup>14</sup> Poly(ethylene glycol)/water has a phase diagram of the closed-loop type with both UCST and LCST. This kind of phase behavior follows from an orientation-dependent interaction (or specific interaction), e.g., a hydrogen bond.<sup>13</sup>

About two decades ago, pulse-induced critical scattering (PICS) was developed to study the onset of phase separation in polymer systems.<sup>15-18</sup> PICS is designed to measure spinodal and cloud points of polymer solutions.

While light scattering yields more detailed information, we are here concerned only with the measurement of phase boundaries. Our work uses a simple, yet precise method for measurement of liquid-liquid phase behavior in polymer/solvent systems; this method is thermo-optical analysis (TOA). We describe a particular TOA apparatus that yields data rapidly and requires only very small samples.

We report here some experimental phase equilibrium data measured with our TOA apparatus. We measure the cloud-point curves of polymer solutions because we plan, at a later time, to compare with results obtained from

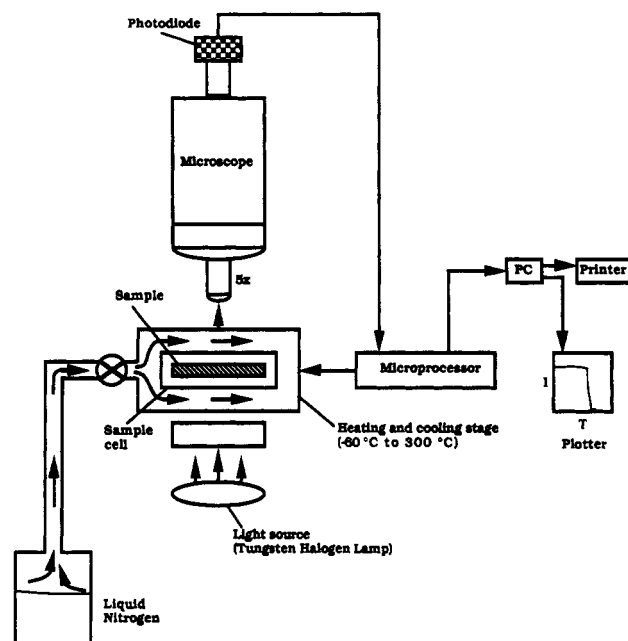


**Figure 1.** Schematic of the apparatus for thermo-optical analysis (TOA).

molecular-thermodynamic models. Consistent with the work of others, we observe an UCST for solutions of polystyrene in cyclohexane, a LCST for solutions of polystyrene in ethyl acetate and both LCST and UCST for solutions of polystyrene in *tert*-butyl acetate. We obtain phase diagrams of the closed-loop type with solutions of poly(ethylene glycol) in water. All of these results were obtained primarily to indicate the reliability of our TOA apparatus.

## Experimental Section

**Materials.** Poly(ethylene glycol) samples were obtained from Union Carbide Corp. for molecular weights 3350 and 8000, from Polysciences, Inc. for molecular weight 15 000, and from Scientific Polymer Products, Inc. for molecular weight 100 000. Their polydispersity indexes ( $M_w/M_n$ ) are shown in Table I. Polystyrene samples were obtained from Pressure Chemical Co. and their polydispersity indexes are listed in Tables II-V. In this study, HPLC grade solvents were used without further purification.

**Sample Preparation.** Samples were prepared in separate test tubes. The composition of each sample was precisely measured gravimetrically. The weight fraction of polymer ranged from 0.005 to 0.55 for the poly(ethylene glycol)/water system,

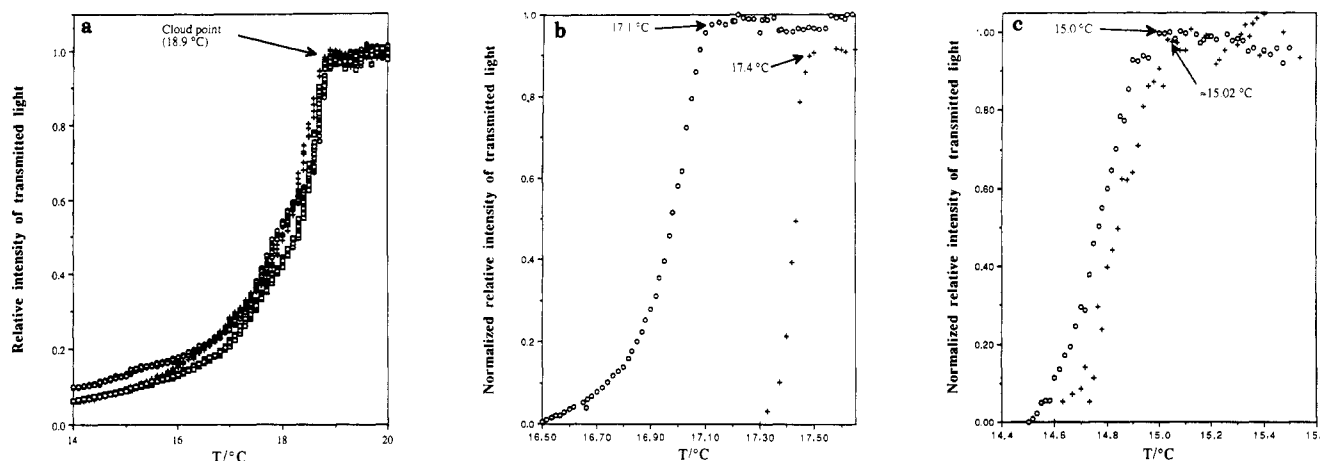


**Figure 2.** (a) Cloud-point determination by TOA for a polymer solution (polystyrene/cyclohexane system;  $M_w/M_n < 1.06$ ; MW = 100 000) with different cooling rates. Circles, crosses, and squares for 0.1, 0.3, and 0.5 °C/min, respectively. (b) Supercooling in cloud-point determination by TOA for a concentrated solution of polystyrene in cyclohexane. ( $W_2 = 0.35$ ; MW = 100 000) with a scan rate 0.1 °C/min. Circles, cooling; crosses, heating. (c) Supercooling in cloud-point determination by TOA for a dilute solution of polystyrene in cyclohexane. ( $W_2 = 0.0045$ ; MW = 100 000) with a scan rate 0.1 °C/min. Circles, cooling; crosses, heating.

**Table I**  
Experimental Cloud-Point Data for Poly(ethylene glycol) in Water<sup>a</sup>

MW = 3350 ( $M_w/M_n \sim 1.6$ )			MW = 8000 ( $M_w/M_n \sim 1.6$ )		
$W_2$	$T_L$ , °C	$T_U$ , °C	$W_2$	$T_L$ , °C	$T_U$ , °C
0.049	157.6	240.5	0.012	132.2	275.5
0.070	156.2	244.9	0.020	128.9	279.0
0.100	155.7	245.4	0.030	126.7	280.9
0.150	155.5	246.4	0.049	124.8	281.9
0.200	156.6	244.6	0.100	124.6	282.5
0.297	158.1	239.8	0.199	124.8	
0.399	164.9	228.5	0.300	128.6	278.9
0.443	172.3	223.2	0.400	136.1	271.2
			0.476	145.2	
			0.550	166.6	230.0

MW = 15 000 ( $M_w/M_n = 1.2$ )			MW = 100 000 ( $M_w/M_n \sim 2.0$ )	
$W_2$	$T_L$ , °C	$T_U$ , °C	$W_2$	$T_L$ , °C
0.002	135.6	270.0	0.005	103.7
0.005	130.0	277.6	0.007	101.5
0.007	128.4	280.2	0.010	102.4
0.010	125.8	284.6	0.030	102.6
0.021	123.2	287.5	0.050	104.3
0.031	121.7		0.070	105.3
0.050	120.2	295.1	0.100	106.4
0.071	119.8	296.1		
0.101	119.5	295.9		
0.202	120.2	295.7		
0.294	124.2	291.8		
0.403	132.9	282.5		
0.501	146.3	266.1		

<sup>a</sup>  $W_2$ , weight fraction of polymer;  $T_L$ , lower consolute temperature;  $T_U$ , upper consolute temperature. Uncertainty in  $W_2$ ,  $\pm 0.0005$ ; uncertainty in  $T$ ,  $\pm 0.05$  °C.

from 0.005 to 0.4 for the polystyrene/cyclohexane system, from 0.005 to 0.3 for the polystyrene/*tert*-butyl acetate system, and from 0.002 to 0.5 for the polystyrene/ethyl acetate system. Each solution was stirred for  $\sim 3$  h. The solution was then transferred to a pyrex tube (i.d. = 1 mm and o.d. = 3 mm). In a conventional sealing method, the test tube is usually sealed under dry nitrogen gas.

We used a filling method similar to that described by Malcolm and Rowlinson.<sup>24</sup> The sample tube was first connected to a vacuum pump and evacuated. The tube was then collapsed and sealed by a vacuum when one end was heated by a flame while the content of the tube was maintained at subambient temperature by liquid nitrogen. A natural gas/oxygen flame was used for sealing. Its temperature was high enough to seal a pyrex tube in less than 2 s. Using this method, we avoid volatilization and

**Table II**  
Experimental Cloud-Point Data for Polystyrene in Cyclohexane<sup>a</sup>

MW = 20 400 ( $M_w/M_n = 1.06$ )		MW = 100 000 ( $M_w/M_n = 1.06$ )		MW = 610 000 ( $M_w/M_n = 1.07$ )	
$W_2$	$T_U$ , °C	$W_2$	$T_U$ , °C	$W_2$	$T_U$ , °C
0.005	3.1	0.005	15.3	0.005	27.3
0.010	4.0	0.010	16.9	0.010	28.0
0.029	4.5	0.030	19.8	0.020	28.1
0.048	4.9	0.049	20.3	0.029	28.3
0.069	6.0	0.063	20.8	0.049	28.0
0.147	6.6	0.081	20.8	0.069	27.6
0.204	6.6	0.103	20.6		
0.293	5.9	0.144	20.5		
0.400	4.5	0.197	19.9		
		0.300	18.3		

<sup>a</sup> For definitions, see Table I.

contamination of the sample. The cloud-point curves were determined at the saturated vapor pressure of solvent.

**Apparatus.** Figure 1 shows the experimental apparatus. It consists of a polarizing microscope (Nikon Optiphot-Pol), a heating-cooling stage, a photodiode (Mettler FP 82), and a microprocessor (Mettler FP 80). An IBM PC was used for data acquisition.

The heating-cooling stage is designed for observation of the thermal behavior of a sample under the microscope. Luminosity in the observation field is measured by a photodiode and recorded on the PC. The temperature program for the given run is entered into the microprocessor. This program consists of a starting temperature, a heating and cooling rate, and an end temperature. Results shown on the microprocessor display are connected to the PC for data storage. The temperature of the system can be varied from  $-60$  to  $+300$  °C with scan rates as low as 0.1 °C/min for both heating and cooling. For experiments below room temperature, the stage coolant inlet is connected to a cooling coil immersed in liquid nitrogen. The coolant air passes through the inlet to the fan and is blown sideways between the external and internal housing of the stage. In the stage, sample temperature is controlled by both the upper and lower plates, assuming symmetric heat distribution through the sample. In this way, equilibrium time can be shortened since the sample cell is directly in contact with the heating unit and the amount of sample is only  $\sim 0.02$  mL. Temperature, measured by a platinum resistance thermometer, is stored on a PC. The observation aperture is covered by a heat-protection filter to prevent damage of microscope parts and heat loss at high temperatures. The photodiode quantitatively measures the intensity of the transmitted light as a function of temperature; these data are used to determine the cloud points of polymer solutions.

Table III  
Experimental Cloud-Point Data for Polystyrene in *tert*-Butyl Acetate<sup>a</sup>

MW = 100 000 ( $M_w/M_n = 1.06$ )			MW = 233 000 ( $M_w/M_n = 1.06$ )			MW = 600 000 ( $M_w/M_n = 1.10$ )		
$W_2$	$T_L$ , °C	$T_U$ , °C	$W_2$	$T_L$ , °C	$T_U$ , °C	$W_2$	$T_L$ , °C	$T_U$ , °C
0.005	165.5	-32.5	0.005	139.9	-12.8	0.005	124.9	-2.7
0.010	160.0	-28.2	0.010	136.1	-8.6	0.010	121.4	0.4
0.030	152.5	-22.6	0.031	130.4	-4.1	0.021	118.8	3.9
0.050	149.8	-20.5	0.051	130.2	-3.7	0.030	118.4	5.5
0.071	150.0	-19.6	0.071	130.0	-2.9	0.051	117.9	4.2
0.101	148.9	-18.5	0.102	130.2	-2.6	0.067	118.6	3.5
0.152	149.3	-17.5	0.151	133.3	-5.9	0.101	121.0	1.7
0.202	150.1	-20.1	0.191	136.1				
0.300	162.0	-26.1						

<sup>a</sup> For definitions, see Table I.

Table IV  
Experimental Cloud-Point Data for Polystyrene in Ethyl Acetate<sup>a</sup>

MW = 100 000 ( $M_w/M_n = 1.06$ )		MW = 233 000 ( $M_w/M_n = 1.06$ )		MW = 600 000 ( $M_w/M_n = 1.10$ )	
$W_2$	$T_L$ , °C	$W_2$	$T_L$ , °C	$W_2$	$T_L$ , °C
0.005	174.5	0.005	159.4	0.002	154.5
0.007	173.2	0.007	158.5	0.007	150.5
0.010	171.5	0.010	156.7	0.010	150.2
0.020	168.0	0.020	154.2	0.020	148.6
0.049	165.5	0.031	153.5	0.030	147.2
0.069	164.4	0.051	151.8	0.039	147.5
0.102	164.6	0.070	152.7	0.050	147.7
0.149	164.6	0.098	153.3	0.069	148.5
0.196	166.1	0.149	155.2		
0.299	173.3	0.200	159.0		
0.489	199.2				

<sup>a</sup> For definitions, see Table I.

Table V  
Experimental Cloud-Point Data for Polystyrene/Methyl Acetate<sup>a</sup>

MW = 770 000 ( $M_w/M_n = 1.04$ )			MW = 770 000 ( $M_w/M_n = 1.04$ )		
$W_2$	$T_L$ , °C	$T_U$ , °C	$W_2$	$T_L$ , °C	$T_U$ , °C
0.003	129.35	28.10	0.039	124.80	32.30
0.008	125.00	30.45	0.068	125.35	27.00
0.018	124.55	32.70	0.078	125.80	26.10

<sup>a</sup> For definitions, see table I.

**Procedure.** A sealed sample tube was placed and centered in the microscope heating-cooling stage and the photodiode with the light source of the microscope was calibrated for the following measurement. To find the range of cloud points of the sample, a high scan rate of heating or cooling (5 °C/min) was used. In this way, the approximate cloud point of the sample was found. The sample was then repeatedly heated or cooled over a temperature range near the cloud point with a low scan rate (0.1 °C/min) while the intensity of light was monitored. The photodiode permitted quantitative determination and recording of the light intensity of the field of view as a function of temperature. Each measurement was repeated at least three times to assure reproducibility.

Figure 2a shows a typical result for cloud-point determination of a polystyrene/cyclohexane system by cooling a sample of known polymer concentration using three different cooling rates (0.1, 0.3, and 0.5 °C/min). All three curves show the same cloud point. The intensity of transmitted light was determined as a function of temperature. Measurements were recorded and stored by the TOA and the data acquisition system. The first phase separation observed (corresponding to the point of abrupt transition of luminosity) was then recorded as the cloud point of the sample at the given concentration.

**Supercooling.** It is important to check for possible supercooling in the determination of cloud-point curves. A static experiment has been performed according to the following procedure. We chose two different concentrations ( $W_2 = 0.0045$  and 0.35) for the polystyrene/cyclohexane system and then the

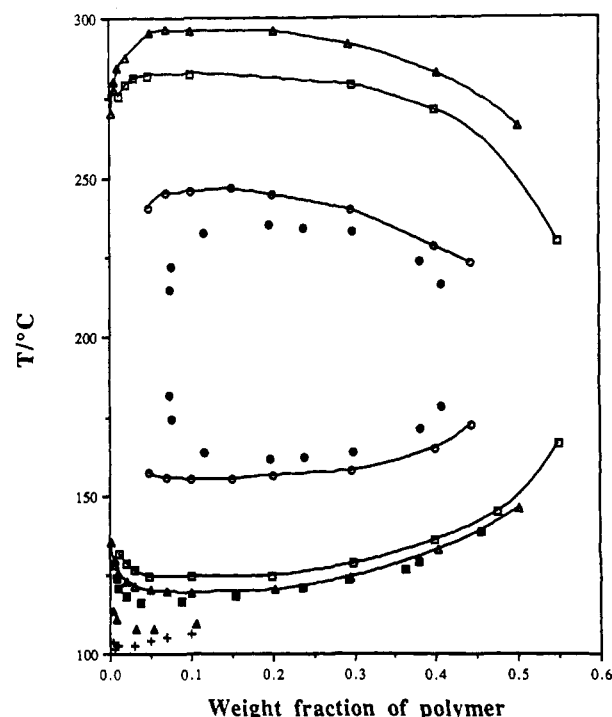
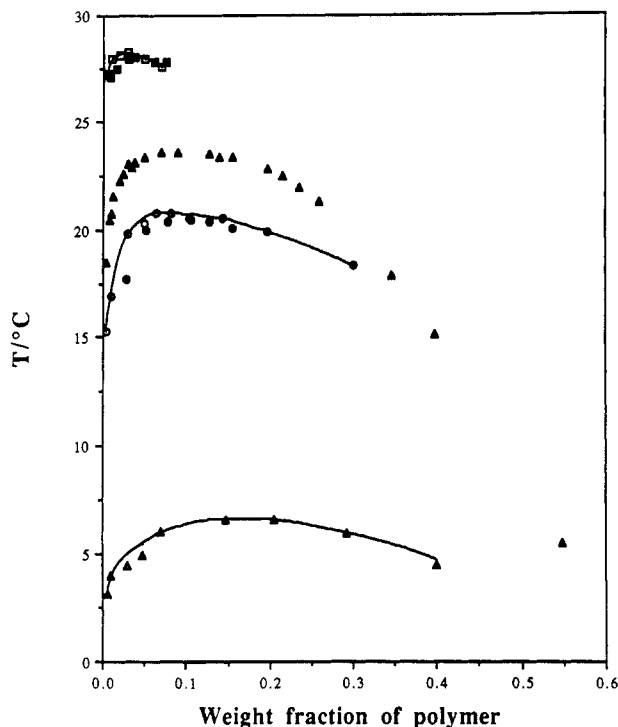


Figure 3. Phase diagrams for several poly(ethylene glycol)/water systems showing cloud-point temperatures as functions of the weight fraction of poly(ethylene glycol). Circles and squares are for molecular weights  $3.35 \times 10^3$  and  $8.0 \times 10^3$ , respectively. Triangles and crosses are for molecular weights  $15 \times 10^3$  and  $100 \times 10^3$ , respectively. Dark symbols are data from Saeki et al.<sup>14</sup> Dark circles, dark squares, and dark triangles are for molecular weights  $3.29 \times 10^3$ ,  $8 \times 10^3$ , and  $14.4 \times 10^3$ , respectively.

cloud point of each concentration was examined by cooling (from heterogeneous to homogeneous) and heating (from homogeneous to heterogeneous) with the same scan rate (0.1 °C/min). At high polymer concentration, the deviation was  $\sim 0.3$  °C, while at low concentration, the deviation was less than 0.1 °C, as shown in Figure 2b and 2c. Koningsveld and Staverman<sup>19</sup> reported that their supercooling effect was 0.6 °C with a scan rate of 1.0 °C/h. Derham et al.<sup>15</sup> showed that PICS was able to minimize the supercooling effect. They reported that the supercooling effect in the low-temperature region was more serious than that in the high-concentration region.

**Advantages of Our TOA Apparatus.** In the apparatus described here, equilibrium is attained rapidly first, because the sample is very small (0.02 cm<sup>3</sup>) and, second, because the sample is in direct contact with the heater or cooler. In conventional TOA systems, equilibrium is not attained as rapidly because the sample is  $\sim 1$  order of magnitude larger and because heat transfer must go through a bath containing the sample.

Data reduction is fast due to the electronic instrumentation shown in Figure 1. Once the apparatus is set up, and after the operator has obtained some experience, it is easily possible to determine the upper and lower cloud-point curves for a binary system in an 8-h day.



**Figure 4.** Phase diagrams for three polystyrene/cyclohexane systems showing cloud-point temperatures as functions of the weight fraction of polystyrene. Squares, circles, and triangles are for molecular weights  $610 \times 10^3$ ,  $100 \times 10^3$ , and  $20.4 \times 10^3$ , respectively. Dark squares and dark circles (Saeki et al.<sup>2</sup>) are for molecular weights  $670 \times 10^3$  and  $97 \times 10^3$ , respectively. Dark triangles are from Shultz and Flory<sup>1</sup> and molecular weight  $89 \times 10^3$ .

## Results and Discussion

Tables I–V give experimental results. Figure 3 shows phase diagrams for poly(ethylene glycol)/water systems for molecular weights  $3.35 \times 10^3$ ,  $8 \times 10^3$ ,  $15 \times 10^3$ , and  $100 \times 10^3$ . Typical closed-loop behavior is observed. The LCST is lowered and the UCST is raised when polymer molecular weight rises. For the highest molecular weight sample ( $100 \times 10^3$ ), only a lower consolute temperature is detected, but we expect that an upper consolute temperature would also exist, provided the poly(ethylene glycol) (PEG) does not degrade thermally before reaching the cloud point. For a monodisperse sample dissolved in a single solvent (a binary system), the cloud-point curve coincides with the binodal and the maximum cloud point is the critical point. However, these features do not hold for solutions of most polymers because of polymer polydispersity. The phase behavior of a mildly polydisperse polymer solution is conveniently analyzed as a quasi-binary system, as discussed by many researchers.<sup>19–23</sup> Stockmayer<sup>25</sup> showed that the critical point of polymer solution depends on both weight- ( $M_w$ ) and z-average molecular weights ( $M_z$ ). However, we do not know the  $M_z$  of our polymer samples. In our study, we are interested in essentially monodisperse polymers. Therefore, the ratio  $M_w/M_n$  is sufficient for our purposes. Although the maximum points of the cloud-point curves for poly(ethylene glycol)/water systems deviate slightly from the critical points, depending on the polydispersity of the samples, the deviation must be small since the samples used in this study are nearly monodisperse. We compared our data with those of Saeki et al.<sup>14</sup> shown in Figure 3. For low molecular weights of PEG, our data show good agreement with the earlier results. However, for high molecular weights of PEG, there is a deviation, probably

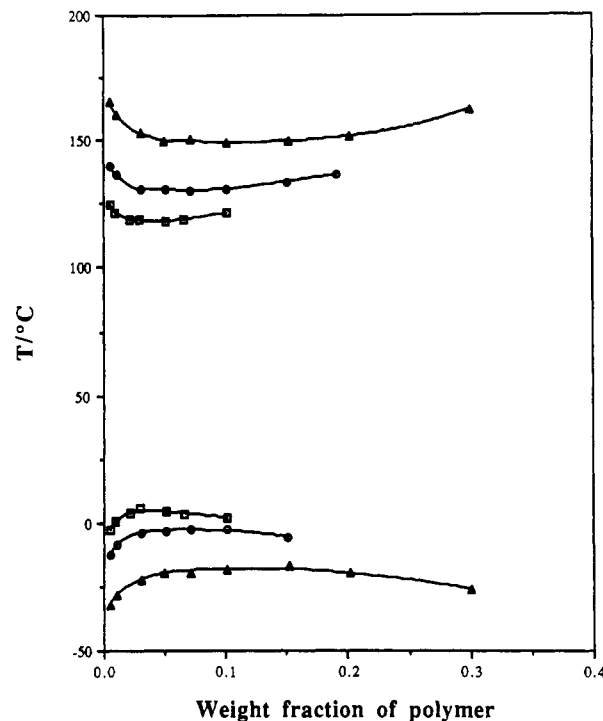


**Figure 5.** Phase diagrams for three polystyrene/*tert*-butyl acetate systems showing cloud-point temperatures as functions of the weight fraction of polystyrene. Squares, circles, and triangles are for molecular weights  $600 \times 10^3$ ,  $233 \times 10^3$ , and  $100 \times 10^3$ , respectively.

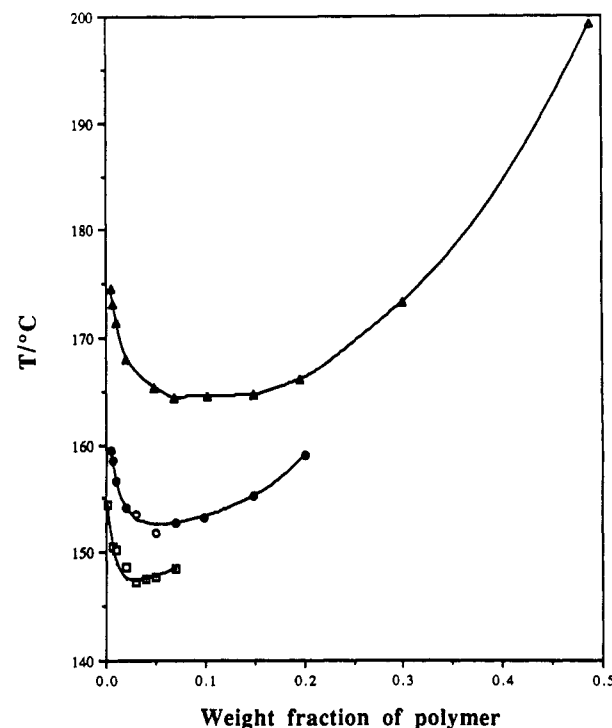


**Figure 6.** Phase diagrams for three polystyrene/ethyl acetate systems showing cloud-point temperatures as functions of the weight fraction of polystyrene. Squares, circles, and triangles are for molecular weights  $600 \times 10^3$ ,  $233 \times 10^3$ , and  $100 \times 10^3$ , respectively.

because the samples studied by others are different from ours (different polydispersity of polymer). TOA was able to detect the upper consolute temperatures of higher molecular weights of PEG ( $M_w = 8000$ ,  $15\,000$ ). The data of Malcolm and Rowlinson<sup>24</sup> show a serious deviation from both our data and those of Saeki et al.<sup>14</sup>

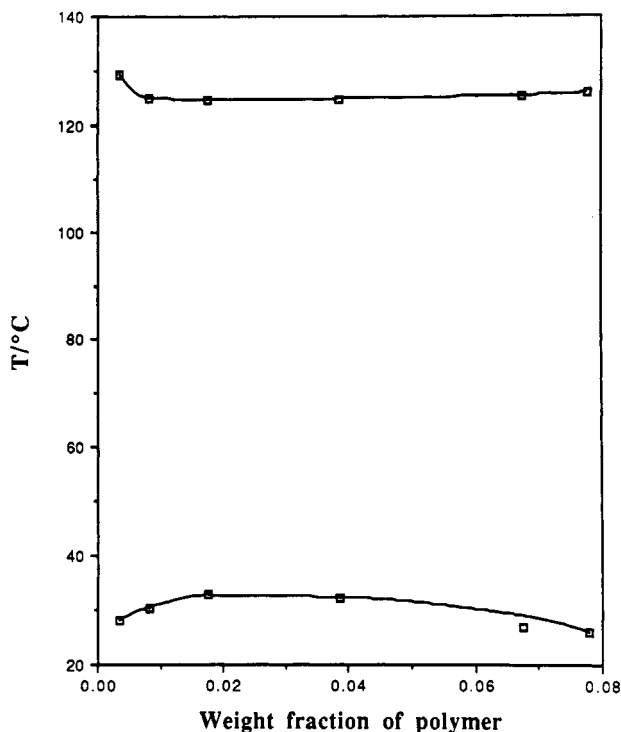


Figure 7. Phase diagram for a polystyrene/methyl acetate system showing cloud-point temperatures as functions of the weight fraction of polystyrene. Molecular weight of polystyrene is  $770 \times 10^3$ .

Saeki et al.<sup>14</sup> reported that the pressure dependence of the cloud points of poly(ethylene glycol)/water systems is insensitive up to 50 atm. The values of  $(dT/dP)$  up to 50 atm for the LCST were shown to be negligibly small. In our study we assume that the system is essentially at the saturated vapor pressure of the solvent.

Figure 3 shows that the width of the closed loop depends on the chain length of PEG. Eventually, a cloud-point curve will disappear at low molecular weights of PEG. Kjellander and Florin<sup>26</sup> reported that, for the PEG/water system, this disappearance occurs at a degree of polymerization of  $\sim 48$ .

Figure 4 shows the cloud-point curves for the polystyrene/cyclohexane systems using molecular weights  $20.4 \times 10^3$ ,  $100 \times 10^3$ , and  $610 \times 10^3$ . The UCST rises with increasing molecular weight, as expected.

Figure 4 shows cloud-point curves of polystyrene in cyclohexane. We measured only the upper consolute temperatures of this system because this "standard" system allows us to compare our results with those in the literature.<sup>1,2</sup> The cloud-point data of Shultz and Flory are slightly higher than ours, while those of Saeki et al.<sup>2</sup> show very good agreement with ours. A slight disagreement may occur because the polymers used in each study are fractionated differently and have different polydispersities.

Figure 5 shows the cloud-point curves of polystyrene in *tert*-butyl acetate. This system exhibits both LCST and UCST. Figure 5 also shows that the UCST is raised and the LCST is lowered with increasing polymer molecular weight. For this system, the temperature region of complete polymer/solvent miscibility is narrowed as molecular weight rises. We do not expect this system to show an hourglass shape for the cloud-point curve. If a poor solvent is chosen, we expect that an increase in molecular weight could cause the UCST and LCST to coalesce, such that the two regions of limited miscibility merge to give an hourglass shape.<sup>13</sup>

Figure 6 shows the cloud-point curves of polystyrene in ethyl acetate. For this system only an LCST is detected, but we expect that an UCST also exists. Figure 7 shows both UCST and LCST of polystyrene in methyl acetate.

## Conclusions

We have used a small-sample TOA apparatus to measure cloud-point curves for several polymer solutions. Our TOA apparatus provides a simple and rapid method to measure both LCST and UCST for polystyrene solutions and closed-loop phase diagrams for aqueous solutions of poly(ethylene glycol). The TOA apparatus described here provides a convenient experimental technique for the determination of liquid-liquid equilibria in binary polymer/solvent systems when the polymer is essentially monodisperse.

**Acknowledgment.** This work was supported by the Director, Office of Energy Research, Office of Basic Energy Sciences, Chemical Sciences Division of the U.S. Dept. of Energy under Contract DE-AC03-76SF00098. This work was also supported by E. I. du Pont de Nemours & Co., Montedipe s.r.l., Norsolor, and Koninklijke/Shell. We are grateful to Mr. D. Leva for help in the experimental work.

## References and Notes

- Shultz, A. R.; Flory, P. J. *J. Am. Chem. Soc.* **1952**, *74*, 4760.
- Saeki, S.; Kuwahara, N.; Konno, S.; Kaneko, M. *Macromolecules* **1973**, *6*, 246.
- Delmas, G.; Patterson, D. *Polymer* **1966**, *7*, 513.
- Cowie, J. M. G.; Maconnachie, A.; Ranson, R. J. *Macromolecules* **1971**, *4*, 57.
- Fox, T. G.; Flory, P. J. *J. Am. Chem. Soc.* **1951**, *73*, 1909.
- Liddell, A. H.; Swinton, F. L. *Discuss. Faraday Soc.* **1970**, *49*, 115.
- Freeman, P. I.; Rowlinson, J. S. *Polymer* **1960**, *1*, 20.
- Orwoll, R. A.; Flory, P. J. *J. Am. Chem. Soc.* **1967**, *89*, 6822.
- Allen, G.; Baker, C. H. *Polymer* **1965**, *6*, 181.
- Polymer Handbook*, 3rd ed; Brandrup, J., Immergut, E. H., Ed.; Wiley Interscience: New York, 1989; Chapter VII.
- Encyclopedia of Polymer Science and Engineering*; Mark, H. F., Ed.; John Wiley and Sons: New York, 1985; Vol. 15.
- Schultz, G. V.; Baumann, H. *Makromol. Chem.* **1963**, *60*, 120.
- Siow, K. S.; Delmas, G.; Patterson, D. *Macromolecules* **1972**, *5*, 29.
- Saeki, S.; Kuwahara, N.; Nakata, M.; Kaneko, M. *Polymer* **1976**, *17*, 685.
- Derham, K. W.; Goldsbrough, J.; Gordon, M. *Pure Appl. Chem.* **1974**, *38*, 97.
- Gordon, M.; Irvine, P.; Kennedy, J. W. *J. Polym. Sci., Polym. Symp.* **1977**, *61*, 221.
- Galina, H.; Gordon, M.; Irvine, P.; Kleintjens, L. A. *Pure Appl. Chem.* **1982**, *54*, 365.
- Galina, H.; Gordon, M.; Ready, B. W.; Kleintjens, L. A. In *Polymers in Solution*; Forsman, W. C., Ed.; Plenum Press: New York, 1986.
- Koningsveld, R.; Staverman, A. J. *J. Polym. Sci., A-2* **1968**, *6*, 349.
- Koningsveld, R.; Staverman, A. J. *J. Polym. Sci., A-2* **1968**, *6*, 305, 325.
- Kurata, M. *Thermodynamics of Polymer Solutions*; Harwood Academic Publishers: New York, 1982.
- Solc, K.; Kleintjens, L.; Koningsveld, R. *Macromolecules* **1984**, *17*, 575.
- Solc, K. *Macromolecules* **1986**, *19*, 1166.
- Malcolm, G. N.; Rowlinson, J. S. *Trans. Faraday Soc.* **1957**, *53*, 921.
- Stockmayer, W. H. *J. Chem. Phys.* **1949**, *17*, 588.
- Kjellander, R.; Florin, E. *J. Chem. Soc., Faraday Trans.* **1981**, *77*, 2053.